PAPER

Accumulation of beryllium and its effects on hydrogen retention in tungsten divertor

To cite this article: Zhihai He *et al* 2018 *Nucl. Fusion* **58** 106015

IOP Publishing | International Atomic Energy Agency Nuclear Fusion

Nucl. Fusion **58** (2018) 106015 (9pp) https://doi.org/10.1088/1741-4326/aad4f3

Accumulation of beryllium and its effects on hydrogen retention in tungsten divertor

Zhihai He[1], H.Y. He[1], J.L. Chen[3], R. Ding[3] and B.C. Pan[1,2,a]

[1] Key Laboratory of Strongly-Coupled Quantum Matter Physics, Department of Physics, University of Science and Technology of China, Hefei, Anhui 230026, People's Republic of China
[2] Hefei National Laboratory for Physical Sciences at Microscale, University of Science and Technology of China, Hefei, Anhui 230026, People's Republic of China
[3] Institute of Plasma Physics, Chinese Academy of Sciences, Hefei 230031, People's Republic of China

E-mail: bcpan@ustc.edu.cn

Received 17 April 2018, revised 18 July 2018
Accepted for publication 20 July 2018
Published 3 August 2018

Abstract

Tungsten (W) and beryllium (Be), as superiorly structural materials, may mutually permeate into each other when used as the plasma-facing materials in a fusion reactor, and interact with hydrogen (H) which commonly exists in the fusion environment. By performing first-principles calculations, we investigate the interactions among W, Be and H in W materials. We find that multiple (up to 10) Be atoms can dissolve in W monovacancy to form nBe-V_W complexes, and these complexes can decrease the formation energy of a vacancy nearby, which in turn promotes the growth of nBe-V_W complexes. The presence of the nBe-V_W complexes reduces the retention of H in vacancy. However, we also find that a small amount of Be dissolved in the small-angle tilt grain boundary (GB) has no obvious influence on H retention, while a large amount of Be will promote the growth of cavities in the GB regions. In addition, the adsorbed Be atoms on W (0 0 1) surface are energetically favorable to aggregate together and form a monolayer structure. The presence of Be atomic layer can weaken the adsorption of H on W surface. This work provides a fundamental insight for understanding the accumulation of Be in W, as well as its effects on H retention. This work did not deal with the case relevant to the Be–W alloying phase, which requires further study.

Keywords: plasma facing materials, tungsten, beryllium, hydrogen, first-principles calculations

(Some figures may appear in colour only in the online journal)

1. Introduction

Controlled thermonuclear fusion is believed to be one of the most promising solutions to the energy crisis, and its application relies on the development of key materials, especially plasma-facing materials. In the current international thermonuclear experimental reactor (ITER), tungsten (W) is chosen to act as the divertor and beryllium (Be) is used as first-wall material [1, 2]. Due to the plasma–wall interactions, the eroded Be impurities may enter into the plasma, resulting in a high Be plasma concentration in the divertor region [3]. The transport and subsequent re-deposition of Be impurities on W divertor will lead to mixing of the materials and may yield Be–W alloys, such as Be_2W and $Be_{12}W$ [4–11]. What's more, it is observed that the existence of Be can suppress the formation of hydrogen (H) bubbles in W [9, 12].

Many theoretical studies have focused on this finding [2, 10, 11, 13–18]. By using molecular dynamics simulation, Lasa *et al* [10] studied the irradiation of Be on W surface at different impacting energies (10–200 eV) and angles (0–75°), and showed that no crystalline alloy structure formed in the W–Be mixed layers after annealing. Moreover, the effect of deuterium co-implanted with Be into W have also been investigated [11]. Based on first-principles calculations, Allouche *et al* [13–15] studied the adsorption of Be atoms on W surface and W atoms on Be surface aiming to elucidate the formation of Be–W alloys, and found that Be atoms can adsorb on W surface with the lower binding energy compared to that in

[a] Author to whom any correspondence should be addressed.

the Be metal. Recently, Zhou *et al* [18] systematically investigated the interaction among W, Be and H, and found that H retention in W can be suppressed by Be doping. However, the first-principles studies above are mainly focused on the interaction of a single Be atom with W and H. Amounts of Be atoms dissolved in W bulk or adsorbed on W surface may corrode the structure of W, and may have a great impact on the retention of H in W bulk. Unfortunately, these questions have not been well investigated. Besides, in our previous work, we demonstrated that amounts of H atoms can accumulate in a small-angle tilt grain boundary (GB) of W, and the H bubble can form at the small-angle GB directly [19]. However, the behavior of Be in W GB and its effect on H retention in the W GB are still unclear.

In this paper, we perform first-principles calculations to investigate the interaction between W, Be and H systematically. The W vacancy and the small-angle tilt GB are considered in order to explore the accumulation behaviors of Be and its effects on H retention in these defective regions. Moreover, the adsorption and accumulation of Be on W surface and its influence on H adsorption are also studied.

2. Computational method

The first-principles calculations are performed by using the Vienna *ab initio* simulation package (VASP) [20] with the projector-augmented wave potential method [21–23]. The exchange-correlation between electrons is described using the generalized gradient approximation (GGA) in the Perdew–Burke–Ernzerhof (PBE) form [24]. The energy cutoff of the plane-wave basis set is 350 eV. The supercells composed of $4 \times 4 \times 4$ unit cells are used for simulating the W bulk and W(0 0 1) surface, and their Brillouin zones are sampled with $3 \times 3 \times 3$ and $3 \times 3 \times 1$ k points within the Monkhorst–Pack scheme [25], respectively. To model the W (0 0 1) surface, a large-sized supercell consisting of 8 atomic layers is employed, in which the two atomic layers at bottom of the supercell are fixed, and a vacuum region of 15 Å is applied to ensure no interaction between the surface and its image. In our optimization, all structures are fully relaxed until the force on each atom is less than 0.02 eV·Å^{-1}. The climbing image nudged elastic band (CI-NEB) method [26] is used to determine the minimum energy paths for diffusion of H or Be atom.

3. Results and discussion

In a fusion environment, W divertor will suffer the irradiation of eroded Be impurity due to the plasma-wall interactions. Most of the impurity Be atoms are deposited on the W surface, while a part of the higher energy Be atoms may permeate into the W bulk. To have a clear understanding of the W–Be interactions as well as the impact of Be on H retention, it is necessary to study the behavior of Be in W bulk and surface. For simplicity, we study the dissolution and accumulation of Be in the W bulk and surface, respectively.

3.1. Dissolution of Be in W bulk

We begin with the dissolution of a single Be atom in W bulk. The solution energy of a Be atom is defined as:

$$E_{\mathrm{sol}}^{\mathrm{Be}} = E_{m\mathrm{W+Be}} - E_{m\mathrm{W}} - E_{\mathrm{Be}}, \quad (1)$$

where $E_{m\mathrm{W+Be}}$ and $E_{m\mathrm{W}}$ are the total energies of the W supercell ($m = 128$) with and without a Be atom, respectively, E_{Be} is the energy of a Be atom in perfect Be bulk (hexagonal close packed), which is evaluated to be $E_{\mathrm{Be}} = -3.75$ eV. In the perfect W bulk, according to our calculations, the Be atom prefers to occupy the octahedral interstitial site (OIS) with the solution energy 4.28 eV, which is consistent with the result by Zhou *et al* [18]. Such a high solution energy implies that it is hard for a Be atom to dissolve in the perfect W bulk. However, when a Be atom dissolves in a W monovacancy, the solution energy is −2.34 eV, much lower than that of Be at the OIS. The binding energy of Be atom with monovacancy reaches up to 6.62 eV, suggesting that Be atom has a strong tendency to combine with vacancy. It is worth noting that the binding energy for a single H or He atom with vacancy is calculated to be 1.29 eV and 4.68 eV, respectively, both obviously lower than that of Be with vacancy, which indicates that Be will be energetically more favorable to occupy the vacancy than H and He.

We then investigate the accumulation of Be atoms in a W vacancy. The binding energy of n$^{\mathrm{th}}$ Be atom with vacancy is defined as

$$E_b^{\mathrm{Be}} = E_{(m-1)\mathrm{W}+(n-1)\mathrm{Be}} + E_{m\mathrm{W+Be}} - E_{(m-1)\mathrm{W}+n\mathrm{Be}} - E_{m\mathrm{W}}, \quad (2)$$

where $E_{(m-1)\mathrm{W}+n\mathrm{Be}}$ and $E_{(m-1)\mathrm{W}+(n-1)\mathrm{Be}}$ are the total energies of the system with n and $n-1$ Be atoms in a vacancy (denoted as nBe-V_{W} and $(n-1)$Be-V_{W} complexes), respectively, and $E_{m\mathrm{W+Be}}$ refers to the total energy of the perfect W supercell ($m = 128$) with an octahedral interstitial Be atom. In such a definition, Be atoms are trapped into vacancy one by one, a positive binding energy indicates the Be atom can be trapped while a negative value means a repulsive tendency. The binding energy per Be as a function of the number of Be atoms in monovacancy is plotted in figure 1. It is remarkable that a vacancy can capture up to 10 Be atoms. The binding energy difference between the first and second Be atom is quite large (about 4 eV), and such large energy difference is originated from the fact that the good symmetrical structure with a Be at the center site of the vacancy is broken by another Be atom. Moreover, for the first 6 Be atoms, the binding energies are quite large (above 2.4 eV), and the Be atoms form a stable octahedral structure, as shown in the insets of figure 1. With increment of Be atoms (6th to 10th), the binding energies decrease strikingly, but still maintain positive value. For instance, the binding energy of 10th Be is 1.31 eV, which is even larger than that of the first trapped H atom in vacancy (1.29 eV according to our calculation). Interestingly, when introducing the 11th Be atom close to 10Be-V_{W} complex, we find that one of the W atoms around the 10Be-V_{W} complex moves out of its initial position and becomes a self-interstitial atom. This implies that the presence of nBe-V_{W} complexes

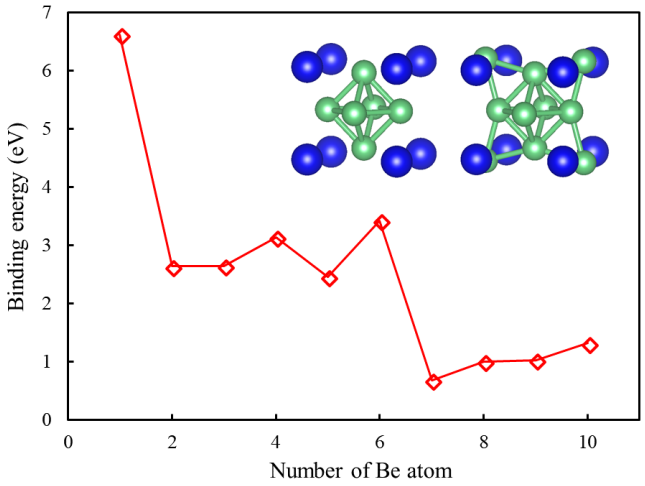

Figure 1. The binding energy per Be as a function of the number of Be atoms in monovacancy. The insets are atomic configurations of the 6Be-V_W and 10Be-V_W complexes, where the blue and green balls represent W and Be atoms, respectively.

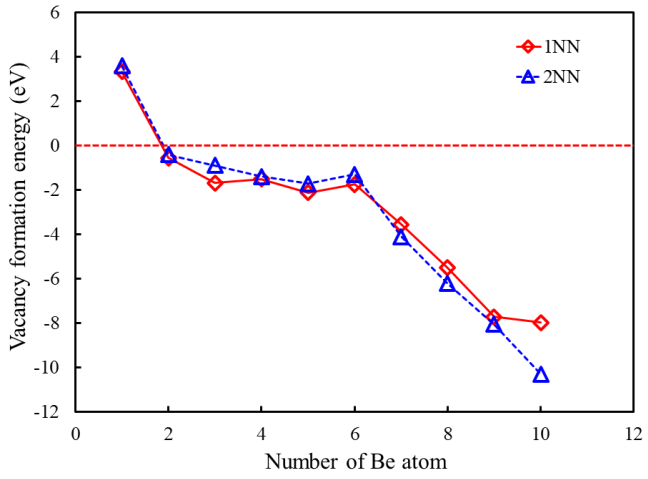

Figure 2. The 1NN and 2NN vacancy formation energies close to nBe-V_W complexes as a function of the number of Be atoms.

may corrode the W atoms around the vacancies, and consequently the vacancies further evolve to be voids.

Inspired by the work of You *et al* [27], we calculate the formation energies of the vacancies around the nBe-V_W complexes via the following definition:

$$E_f^V = E_{(m-2)W+nBe} + E_W - E_{(m-1)W+nBe}, \quad (3)$$

where $E_{(m-1)W+nBe}$ and $E_{(m-2)W+nBe}$ are the total energies of the system with nBe-V_W and nBe-2V_W complexes, respectively, E_W is the energy of a W atom in the prefect W bulk. Here, we systematically calculate the formation energies of the first-nearest-neighbor (1NN) and second-nearest-neighbor (2NN) vacancies around the nBe-V_W ($n = 1$–10) complexes, as displayed in figure 2. The formation energies for 1NN and 2NN vacancies of 1Be-V_W complex are 3.32 and 3.58 eV, respectively, which are very close to that of the vacancy without Be (3.31 and 3.67 eV). However, even two Be atoms are trapped inside the vacancy, the formation energies for 1NN and 2NN vacancies become negative. By checking the configurations, we find that when a new vacancy is introduced around of a 2Be-V_W complex, one of the Be atoms migrates to and occupies the center of this new vacancy, which significantly reduces the total energy of system. As the number of Be atoms increases from 2 to 6, the 1NN and 2NN vacancy formation energies of the nBe-V_W complexes are slowly reduced. Differently, when the number of Be atoms is larger than 6, the vacancy formation energies decrease quickly. Such variation trend demonstrates that the presence of nBe-V_W complexes ($n > 1$) in W reduces the stability of W atoms near the vacancy, and helps the formation of the additional vacancies, especially for $n > 6$. It is worth noting that the reduction of vacancy formation energy around nBe-V_W complexes is more remarkable compared to the case of nH-V_W and nHe-V_W complexes [27].

To have a clear understanding of the stability reduction of W atoms around the nBe-V_W complexes, we calculate the electron-density distributions of the related systems. As shown in figures 3(*a*) and (*b*), for the case of an isolated Be atom dissolved in vacancy, the distribution of electron density changes unobviously, and thus the influence on stability of the surrounding W atoms is slight. However, after 10 Be atoms being captured by vacancy, the change of electron-density distribution is significant, as can be seen in figure 3(*c*). Compared figures 3(*c*) with (*a*) and (*b*), the electron density around *A* and *B* atoms (1NN and 2NN W atoms of vacancy) is apparently higher, which enhances the Coulomb repulsive interaction between *A* and *B* atoms and results in instability of the 1NN and 2NN W atoms around 10Be-V_W complex. The results above can also be confirmed by Bader charge analysis [28]. Owing to the lower electronegativity of Be, part of electrons transfer from Be to W when Be atom dissolves in W. As given in figure 3(*e*), when a Be atom dissolves in vacancy, there are 0.92 electrons transfer from the Be atom to the surrounding W atoms, and the net charge on the *A*, *B* and *C* atoms are −0.06, −0.08 and 0.02 *e*, respectively. Such small amount of charge transfer is not sufficient to significantly change the W–W interactions. With more Be atoms trapped in the vacancy, more electrons transfer to the W atoms. For the case of 10Be-V_W complex (figure 3(*f*)), the net charge on the *A*, *B* and *C* atoms are −0.40, −0.50 and −0.24 *e*, respectively. Consequently, the Coulomb repulsive interactions weaken the bonding of W with its nearest W atoms, and thus reduce the stability of W atoms around the nBe-V_W complexes.

Overall, our study revealed that the stability of W atoms close to the nBe-V_W ($n > 1$) complexes can be drastically reduced, which promotes the accumulation of Be atoms in W vacancies. More seriously, it is possible that the W atom is emitted from the vicinity of the nBe-V_W complexes to become a self-interstitial atom. This may explain the experimental results of Be-rich alloy phases formation, such as Be_2W, $Be_{12}W$ [7, 9]. However, it should be noted that we did not deal with the formation of Be–W alloying phase under present conditions. To simulate the alloying process of W and Be, it is more appropriate by using molecular dynamics simulation or other techniques.

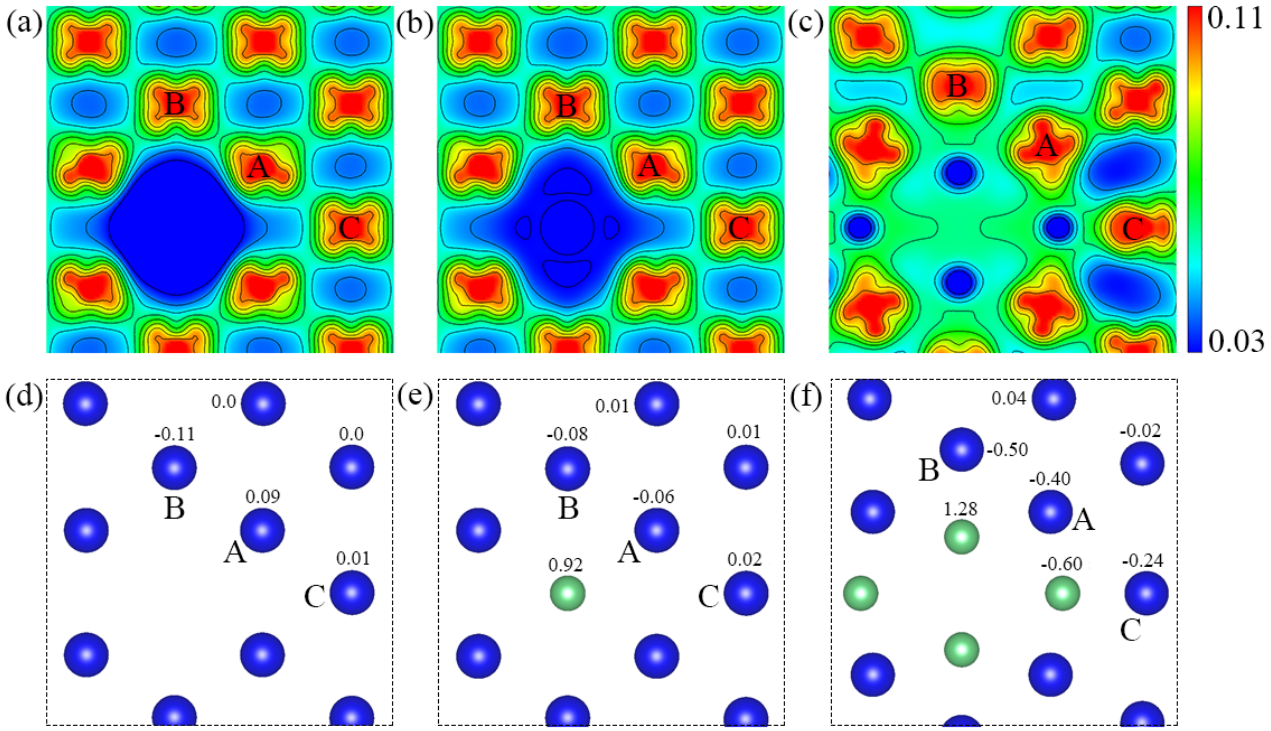

Figure 3. Electron-density distribution (electron/bohr^3) on the (0 1 1) plane in three cases: the monovacancy (*a*), the 1Be-V_W (*b*) and 10Be-V_W (*c*) complex. (*d*), (*e*) and (*f*) are the atomic configurations and Bader charge correspond to (*a*)–(*c*), respectively. The number on each labelled atom represents the net charge (electron) on the atom. *A*, *B* and *C* denote the 1NN, 2NN and 3NN W atoms of the vacancy, respectively.

3.2. Effect of Be on H retention in W bulk

3.2.1. Effect of nBe-V_W complexes. The dissolution behavior of H in the 1Be-V_W complex has been investigated by Zhou *et al* [18], and it was found that the presence of Be can severely weaken the trapping effect of vacancy on H. Since a vacancy can capture multiple Be atoms easily from above, so we thus concern the effect of nBe-V_W complexes on H retention in W bulk in the following.

Like the Be atom trapped by a vacancy, the binding energy of kth H atom with nBe-V_W complexes can be defined as:

$$E_b^H = E_{(m-1)W+nBe+(k-1)H} + E_{mW+H} - E_{(m-1)W+nBe+kH} - E_{mW}, \quad (4)$$

where $E_{(m-1)W+nBe+kH}$ and $E_{(m-1)W+nBe+(k-1)H}$ are the total energies of the nBe-V_W system with k and $k-1$ H atoms, respectively, and E_{mW+H} is the total energy of the perfect W supercell containing a tetrahedral interstitial H atom.

Figure 4 shows the binding energy per H with 1Be-V_W complex as a function of the number of H atoms. Similar to that reported in [18], the binding energy per H atom with 1Be-V_W complex is smaller than that in the monovacancy, indicating that the presence of Be can suppress the dissolution of H in vacancy. However, our result shows that the 1Be-V_W complex is able to trap 7 H atoms at most, differing from the 5 H atoms in [18]. This may be due to a more extensive search for the ground state of each (1Be-kH)-V_W complex in our work. Besides, we use the PBE form of GGA in our calculations, while it is Perdew-Wang functional [29] in the [18]. As multiple H atoms are trapped by 1Be-V_W complex,

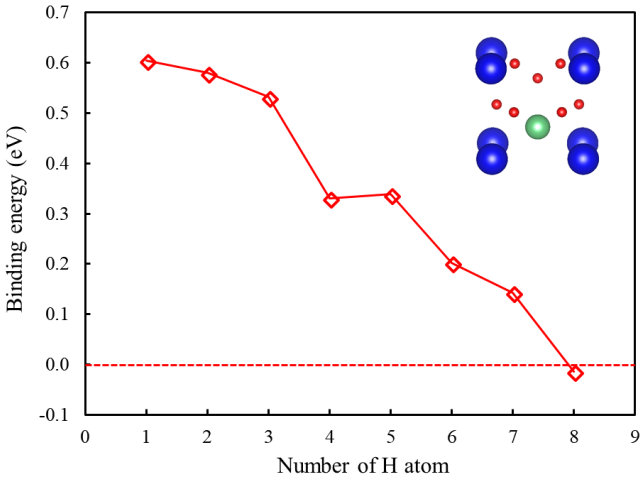

Figure 4. The binding energy per H as a function of the number of H atoms in the 1Be-V_W complex. The inset is the atomic configuration of (1Be-7H)-V_W complex.

the Be atom prefers to occupy the center of vacancy no longer. Indeed, the Be atom and H atoms will occupy one half of the vacancy region spaciously, as shown in the inset of figure 4. This implies the repulsive interaction between Be and H atoms, which is in agreement with the result of Be weakening the trapping effect of vacancy on H.

Considering the repulsive interaction between Be and H atoms, it is reasonable to believe that the dissolving capability of H in vacancy will continue to reduce with more Be atoms being trapped by the vacancy. The binding energy of the first

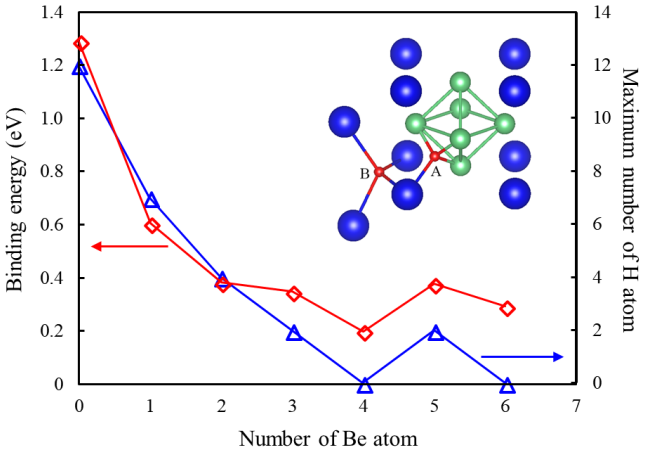

Figure 5. The binding energy of first H (red diamonds) and the maximum number of H atoms (blue triangles) as a function of the number of Be atoms in nBe-V_W complexes. The inset illustrates the H interstitial sites close to 6Be-V_W complex.

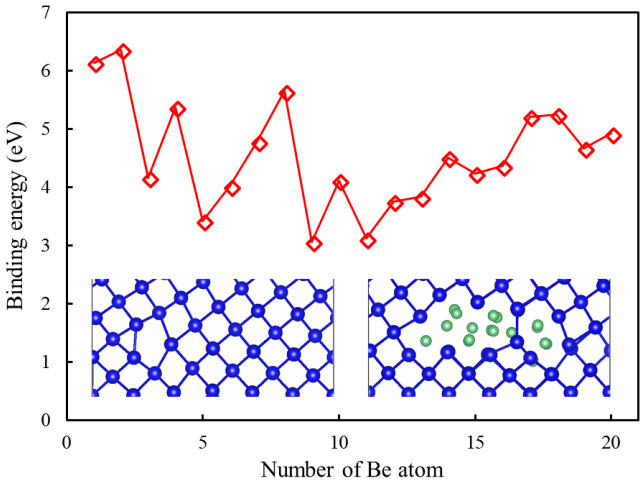

Figure 6. The binding energy per Be as a function of the number of Be atoms in the GB. The insets are the local atomic configurations of the small-angle GB without and with 20 Be atoms, respectively. The lines are used to guide the eyes.

H and the maximum number of H atoms in nBe-V_W complexes as a function of the number of Be atoms are plotted in figure 5. As a whole, the capability of H to dissolve in nBe-V_W complexes decreases with increasing the number of Be atoms. Especially, in the case of 4Be-V_W and 6Be-V_W complexes, the first H atom indeed moves out of the vacancy, so there is no H atom can dissolve in the vacancy. Taking the 6Be-V_W complex for example, there exist two stable sites (A and B) for H around the complex (as displayed in the inset of figure 5), and the solution energies of H at the site A and B are 2.39 and 0.66 eV, respectively. Compared to the solution energy of H at TIS in the perfect W bulk (0.96 eV), the former is much higher, while the latter is slightly lower. In other words, the H atom is energetically favorable to dissolve in the region around the 6Be-V_W complex with a binding energy of about 0.3 eV. It is worth noting that the binding energies of the first H in nBe-V_W complexes ($n > 1$) are smaller than 0.4 eV, such a weak interaction between the H atom and the complexes means that the complexes are hard to contain any H atom at high temperature.

The above results suggest that the H retention in vacancy can be significantly reduced by Be atoms. Compared to a single Be atom, multiple Be atoms combined with vacancy have a stronger inhibiting effect on the H retention in vacancy.

3.2.2. Effect of Be in small-angle GB. Besides vacancies, defects such as dislocations and grain boundaries in metals are usually regarded as nucleation sites for H bubbles. In our earlier work [19], we showed that the small-angle tilt GB can capture a lot of H atoms, resulting in the formation of H bubbles eventually. Taking the blocking effect of nBe-V_W complexes on H retention into account, we wonder that whether the presence of Be atoms can reduce the H retention in W GBs so as to suppress the formation of H bubble on GBs? To answer this question, we use the same model of small-angle tilt GB as in our previous work (a detailed description of structural model and calculation parameters can be found in [19]) to investigate the accumulation of Be atoms and its effects on H retention in GB.

Like a vacancy, the small-angle GB, a transition region between two adjacent single crystal lattices, can also trap multiple Be atoms. As shown in figure 6, the binding energy of the first Be is 6.14 eV, which is close to the binding energy of the first Be in vacancy, implying the strong attractive interaction between the GB and Be. With the increasing number of the trapped Be atoms, the binding energies with fluctuation features are all larger than 3.0 eV, even when the number of Be atoms reaches up to 20 (the related areal density is 1.7×10^{15} Be atoms per cm^2, which is calculated by n/S, here S is the cross-sectional area of the GB). This indicates that the GB has great capacity of capturing Be atoms. As can be seen in the insets of figure 6, the Be atoms weaken the W–W bonds in the GB and lead to expansion of the defective region, which in turn promote the GB to capture more Be atoms. This drops a hint that Be accumulation may have few influence on the formation of H bubble in GB.

We now explore the influence of Be on the formation of H bubble in GB. It was reported previously that H and He can diffuse in W bulk with barriers as small as 0.21 eV [30] and 0.06 eV [31], respectively, while the diffusion barrier of Be in W bulk is much higher (1.13 eV according to our calculation). The Be atoms from irradiation were found mainly deposit on surface or locate in the near-surface layer [9]. So it is reasonable to suppose that there may be only a few Be atoms captured by the GB in real fusion environment, although the small-angle GB exhibits a high ability in trapping Be atoms. Taking for a typical example, we investigate the gathering behaviors of H atoms at the small-angle GB with 4 Be atoms (areal density 3.3×10^{14} Be atoms per cm^2) dissolved in it. The binding energy per H as the function of the number of H atoms in GB with and without Be are plotted in figure 7. We emphasize that in our calculations, the H atoms are introduced into the GB randomly, so the binding energies fluctuate in a broad range. Nevertheless, in both cases, the binding energies are all larger than 0.3 eV, demonstrating that H atoms energetically favor to accumulate in the GB. By examining the local structure of GB, it is found that the trapped H atoms

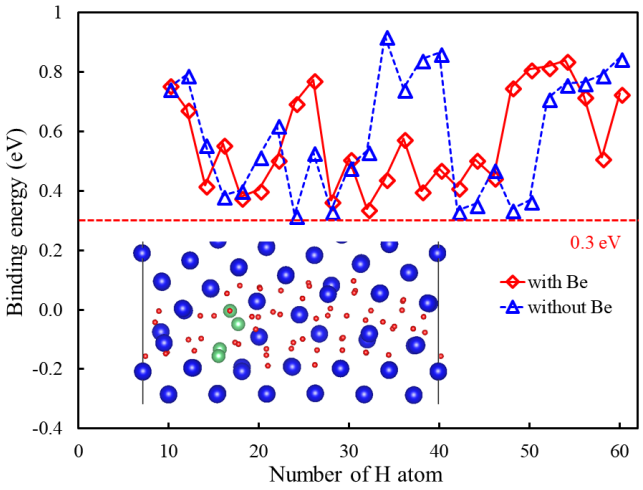

Figure 7. The binding energy per H as a function of the number of H atoms in the GB with and without Be. The inset is the local atomic configuration of the small-angle GB, which containing 4 Be atoms and 60 H atoms. The lines are used to guide the eyes.

would diffuse over the whole region of the GB eventually, as depicted in the inset of figure 7. As a consequence, the accumulation of H atoms ultimately brings about the formation of H bubble at GB, and similar results can be found in the case of GB without Be. These results imply that a small amount of Be atoms dissolved in the small-angle GB cannot suppress the formation of H bubble.

In [12], the author speculated a possible H blister inhibiting mechanisms: a small amount of Be trapped in the grain boundaries may prevent the formation and growth of cavities in these regions. However, this speculation is not supported by our calculations. The presence of several Be (e.g. areal density 3.3×10^{14} Be atoms per cm^2) in small-angle GB has insignificant effect on inhibition of H bubbles, while a large amount of Be (e.g. areal density 1.7×10^{15} Be atoms per cm^2) may promote the growth of cavities in the GB regions. Of course, it should be noted that the results above are obtained from one kind of small-angle tilt GB, the conclusion may not be appropriate for all grain boundaries.

3.3. Adsorption of Be on W (0 0 1) surface

3.3.1. The behavior of Be on W (0 0 1) surface. In a fusion environment, the impurity of Be atoms eroded from the first-wall may transport and subsequently redeposit on the W divertor, to cause mixing of the materials and formation of alloys. As the first step in alloying, the adsorption and accumulation of Be on the W surface is studied in this work.

We chose the adsorption of Be atoms on reconstructed W (0 0 1) surface as the typical case, since the pure reconstructed W (0 0 1) surface has been well investigated by Heinola *et al* [32]. The definition of Be adsorption energy on W surface is the same as formula (1). In the previous work of Allouche *et al* [14, 15], a Be atom prefers to adsorb at a bridge site between two W atoms in W (0 0 1) surface, with adsorption energy of about 1.4 eV. However, it is incompatible with our results. According to our calculations, there are three different stable adsorption sites for Be on the reconstructed W (0 0 1) surface: short bridge (site *A*), long bridge (site *B*) and face centered (site *C*) sites, as shown in figure 8(*a*), and their adsorption energies are 1.34, 1.12 and −0.42 eV, respectively. The adsorption energies of Be at bridge sites are consistent with the result in [14], but it is much higher than that at face centered site. It is worth pointing out that the energy of Be atom dissolving in OIS of W bulk is 4.7 eV higher than Be atom adsorbing on W (0 0 1) surface, indicating that the probability of a Be atom penetrating into W bulk from the surface is very small.

To explore the accumulation behaviors of Be on W surface, we investigate the diffusion behavior of Be atom firstly. According to our calculations, the energy profiles for Be migrating on the W (0 0 1) surface are provided in figure 8(*b*). From figure 8(*b*), we can see that the minimum energy barrier reaches up to 1.54 eV, so the diffusion of a Be atom on W (0 0 1) surface is not easy. Nevertheless, considering the highly complex and extreme irradiation environments, it is not unlikely for Be to diffuse on W surface. Interestingly, it is found that the two transition states in figure 8(*b*) are short bridge and long bridge sites exactly, suggesting that bridge sites are metastable sites for Be adsorbing on W (0 0 1) surface.

Next, we investigate the interaction of Be atoms adsorbed on the W (0 0 1) surface. The binding energies of the adsorbed Be atoms can be obtained by:

$$E_b(n\mathrm{Be}) = nE_{\mathrm{surface+Be}} - E_{\mathrm{surface}+n\mathrm{Be}} - (n-1)E_{\mathrm{surface}}, \quad (5)$$

where $E_{\mathrm{surface+Be}}$ and $E_{\mathrm{surface}+n\mathrm{Be}}$ are the total energies of the supercell with one and n Be atoms on the surface, respectively, and E_{surface} is the total energy of the clean W surface. The binding energies of adsorbed Be atoms are listed in table 1, and the corresponding atomic configurations are shown in figures 8(*d*)–(*f*). Clearly, the binding energy increases with the number of Be atoms, suggesting that the Be atoms adsorbed on W surface have a tendency to aggregate together. This can be understood by the charge transfer. When a Be atom adsorbed on the face centered site, as shown in figure 8(*c*), there are 1.01 electrons transfer from the Be atom to the neighboring W atoms, so that Be can bond with these W atoms. As another Be atom occupies the adjacent face centered site, there exist several common neighboring W atoms, the net charge on these W atoms increase with the number of first-nearest-neighbor Be atoms. For instance, the net charge on the atom *A* in figures 8(*c*)–(*f*) are −0.28, −0.61, −0.96 and −1.35 *e*, respectively. The increased net charge on the W atoms enhances their binding to the neighboring Be atoms. So, the Be atoms prefer to aggregate together when they adsorbed on W (0 0 1) surface. Furthermore, we consider an extreme case: a layer of Be atoms cover the W (0 0 1) surface. In this case, the adsorption energy of an additional Be atom on such surface is 1.10 eV, which is 1.52 eV higher than that of Be atom on clean W (0 0 1) surface. This indicates that the adsorbed Be atoms on W (0 0 1) surface prefer to accumulate as a monolayer firstly.

3.3.2. Interaction of Be and H on W (0 0 1) surface. We further explore the effect of Be on adsorption of H on the W

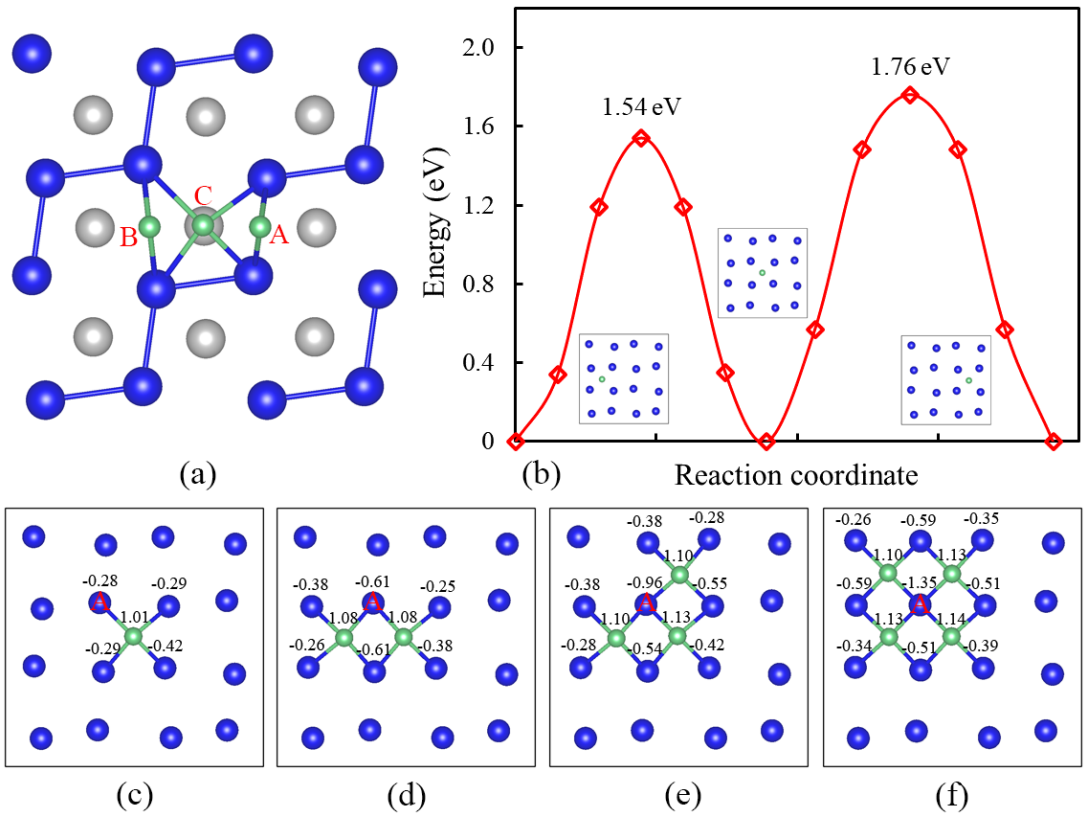

Figure 8. (*a*) Top view of the reconstructed W (0 0 1) surface. The blue and grey balls represent the surface and subsurface W atoms, respectively. The *A*, *B* and *C* green balls denote the potential adsorption sites of Be, corresponding to the short bridge, long bridge and face centered sites, respectively. (*b*) The energy profiles for Be migrating on the reconstructed W (0 0 1) surface. (*c*)–(*f*) The atomic configurations and Bader charge of Be atoms adsorb on W (0 0 1) surface, where the number on each labelled atom represents the net charge (electron) on the atom.

Table 1. The binding energy of Be atoms on the reconstructed W (001) surface.

	2Be	3Be	4Be
E_b (eV)	0.41	0.80	1.41

(001) surface. The adsorption energy of an H atom on W surface can be obtained by:

$$E_{\text{ads}} = E_{\text{surface+H}} - E_{\text{surface}} - 1/2E_{\text{H}_2}, \quad (6)$$

where $E_{\text{surface+H}}$ is the total energy of supercell with one H atom adsorbed on surface, E_{H_2} is the total energy of an H_2 molecule.

On the clean reconstructed W (0 0 1) surface, H prefers to adsorb at the short bridge site with adsorption energy of −0.92 eV, which is 0.46 eV lower than that at long bridge site, being in good consistent with the result by Heinola *et al* [32]. In addition, when two H atoms are adsorbed at adjacent short bridge sites, the binding energy is −0.14 eV, suggesting that there is a repulsive interaction between the H atoms. This implies the formation of H clusters on W (0 0 1) surface is energetically unfavorable.

As shown in figure 9, when a Be atom is adsorbed at the face centered site of W (0 0 1) surface, the adsorption energy of H around the Be atom is slightly higher than that on the clean W surface, suggesting the repulsive interaction between Be and H. Therefore, the single Be atom on the W (0 0 1) surface

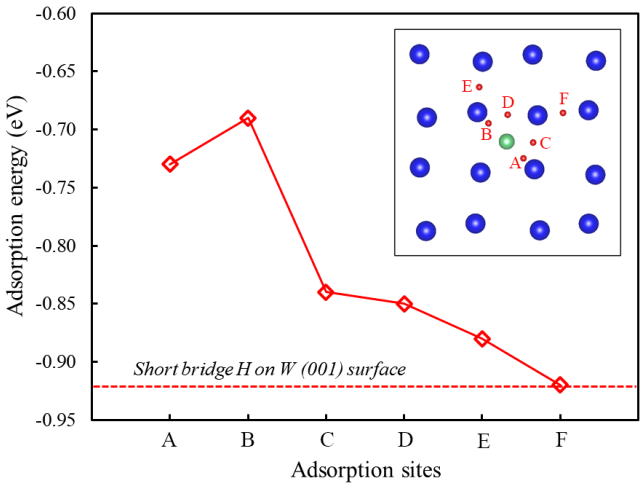

Figure 9. The adsorption energies of H on the W (0 0 1) surface with Be as a function of H sites. A–F represent the adsorption sites of H. The lines are used to guide the eyes.

cannot serve as a trapping center for H. This is different from the case in W bulk, where the interstitial Be and H exhibit a weak attractive interaction [18].

As mentioned above, the adsorbed Be atoms on W (0 0 1) surface prefer to assemble as a monolayer firstly, the Be atomic layer should have some effects on the adsorption of H on W surface. To this end, we further investigate the adsorption and

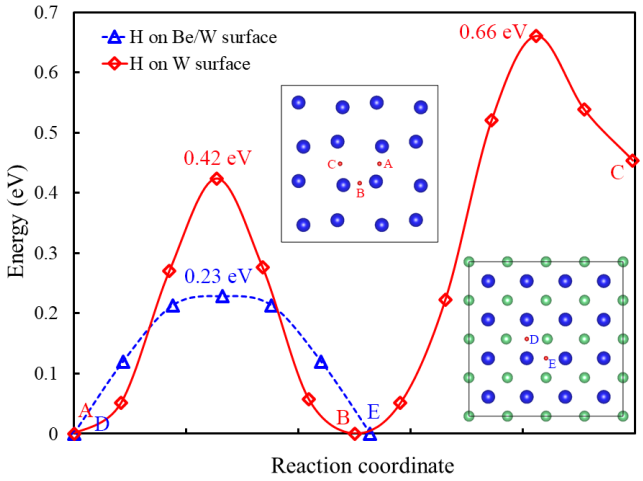

Figure 10. The energy profiles for H migrating on the clean W (001) surface (red line) and the Be/W surface (blue dashed line).

diffusion behavior of H on the W (001) surface, where the surface covered by a layer of Be atoms (we call it 'Be/W surface'). It is found that the adsorption energy of H at the most stable site on Be/W surface is −0.58 eV, which is 0.34 eV higher than that of H on the clean W (001) surface. Hence, the ability of H adsorbed on W surface will be reduced because of the presence of Be atomic layer. In addition, we found that the diffusion of H on the Be/W surface is faster than H on the clean W (001) surface. As clearly shown in figure 10, the diffusion of H on the clean W (001) surface proceeds via the adjacent short bridge sites with an energy barrier of 0.42 eV. However, on the Be/W surface, the barrier of H diffusion decreases to 0.23 eV, which is almost one half of the former. In other words, the presence of Be atomic layer will accelerate the diffusion of H on W (001) surface.

4. Conclusions

Based on first-principles calculations, we have systematically investigated the accumulation of Be and its effect on H retention in W vacancy and small-angle tilt GB, the adsorption and accumulation of Be on the reconstructed W (001) surface are also explored. The main conclusions are:

(1) Multiple Be atoms (up to 10) can dissolve in monovacancy to form nBe-V_W complexes, and the formation energy of the vacancy close to a nBe-V_W complex is remarkably reduced. The reduced vacancy formation energy indicates the stability of W atoms around the nBe-V_W complexes is declined, which will promote the growth of nBe-V_W complexes. What's more, the formation of nBe-V_W complexes can significantly block the retention of H in vacancy and thus reduce the H retention in W bulk.

(2) For the case of small-angle tilt GB, a small amount of Be (e.g. areal density 3.3×10^{14} Be atoms per cm^2) dissolved in the GB has no obvious impact on the inhibition of H bubble, while a large amount of Be (e.g. areal density 1.7×10^{15} Be atoms per cm^2) will promote the growth of cavities in the GB regions.

(3) On the reconstructed W (001) surface, Be atoms prefer to adsorb at face centered site, and the adsorbed Be atoms prefer to aggregate to a monolayer firstly. The presence of Be atomic layer can weaken the adsorption of H on the W (001) surface.

These findings are helpful to understand the nucleation and accumulation of Be in W, as well as its inhibiting effect on H retention.

Acknowledgments

This work is financially supported by the National Magnetic Confinement Fusion Program (Grant No. 2013GB107004), the Fundamental Research Funds for the Central Universities (No. WK3510000005), and the National Natural Science Foundation of China (No. 11105140, 11275191). The computational center of USTC is acknowledged for computational support.

References

[1] Brezinsek S. and JET-EFDA contributors 2015 *J. Nucl. Mater.* **463** 11
[2] Gyoeroek M., Kaiser A., Sukuba I., Urban J., Hermansson K. and Probst M. 2016 *J. Nucl. Mater.* **472** 76
[3] Schmid K., Baldwin M., Doerner R. and Wilthner A. 2004 *Nucl. Fusion* **44** 815
[4] Wiltner A. and Linsmeier C. 2005 *J. Nucl. Mater.* **337–9** 951
[5] Doerner R., Baldwin M. and Causey R. 2005 *J. Nucl. Mater.* **342** 63
[6] Wiltner A. and Linsmeier C. 2006 *New J. Phys.* **8** 181
[7] Baldwin M.J., Doerner R.P., Nishijima D., Buchenauer D., Clift W.M., Causey R.A. and Schmid K. 2007 *J. Nucl. Mater.* **363–5** 1179
[8] Wiltner A., Kost F., Lindig S. and Linsmeier C. 2007 *Phys. Scr.* **T128** 133
[9] Baldwin M.J., Doerner R.P., Nishijima D., Tokunaga K. and Ueda Y. 2009 *J. Nucl. Mater.* **390–1** 886
[10] Lasa A., Heinola K. and Nordlund K. 2014 *Nucl. Fusion* **54** 083001
[11] Lasa A., Heinola K. and Nordlund K. 2014 *Nucl. Fusion* **54** 123021
[12] Doerner R.P., Baldwin M.J., Nishijima D., Roth J. and Schmid K. 2011 *J. Nucl. Mater.* **415** S717
[13] Allouche A. and Linsmeier C. 2008 *J. Phys.: Conf. Ser.* **117** 012002
[14] Allouche A., Wiltner A. and Linsmeier C. 2009 *J. Phys.: Condens. Matter* **21** 355011
[15] Allouche A. 2009 *Chem. Phys. Lett.* **470** 119
[16] Allouche A., Fernandez N. and Ferro Y. 2014 *J. Phys.: Condens. Matter* **26** 315012
[17] Mutzke A., Bandelow G. and Schneider R. 2015 *J. Nucl. Mater.* **467** 413
[18] Zhou H.B., Momanyi N.K., Li Y.H., Jiang W. and Li X.C. 2016 *RSC Adv.* **6** 103622
[19] He Z.H., He H.Y., Ding R., Pan B.C. and Chen J.L. 2016 *Phys. Chem. Chem. Phys.* **18** 33103
[20] Kresse G. and Hafner J. 1993 *Phys. Rev.* B **47** 558
[21] Blöchl P.E. 1994 *Phys. Rev.* B **50** 17953
[22] Kresse G. and Furthmüller J. 1996 *Phys. Rev.* B **54** 11169
[23] Kresse G. and Joubert D. 1999 *Phys. Rev.* B **59** 1758
[24] Perdew J.P., Burke K. and Ernzerhof M. 1996 *Phys. Rev. Lett.* **77** 3865

[25] Monkhorst H.J. and Pack J.D. 1976 *Phys. Rev.* B **13** 5188
[26] Henkelman G., Uberuaga B.P. and Jónsson H. 2000 *J. Chem. Phys.* **113** 9901
[27] You Y.W., Kong X.S., Wu X.B., Liu C.S., Chen J.L. and Luo G.N. 2017 *Nucl. Fusion* **57** 016006
[28] Tang W., Sanville E. and Henkelman G. 2009 *J. Phys.: Condens. Matter* **21** 084204
[29] Perdew J.P. and Wang Y. 1992 *Phys. Rev.* B **45** 13244
[30] Heinola K. and Ahlgren T. 2010 *J. Appl. Phys.* **107** 113531
[31] Becquart C.S. and Domain C. 2006 *Phys. Rev. Lett.* **97** 196402
[32] Heinola K. and Ahlgren T. 2010 *Phys. Rev.* B **81** 073409